Abdominal Radiology

Published online: 27 June 2018

Abdom Radiol (2019) 44:346–354
https://doi.org/10.1007/s00261-018-1678-x

Validation of a DIXON-based fat quantification technique for the measurement of visceral fat using a CT-based reference standard

Katherine M. Heckman,[1] Bamidele Otemuyiwa,[1] Thomas L. Chenevert,[2] Dariya Malyarenko,[2] Brian A. Derstine,[3] Stewart C. Wang,[3,4] and Matthew S. Davenport[2,5,6,7]

[1]University of Michigan Medical School, Ann Arbor, MI, USA
[2]Department of Radiology, Michigan Medicine, Ann Arbor, MI, USA
[3]Morphomics Analysis Group, Michigan Medicine, Ann Arbor, MI, USA
[4]Department of Surgery, Michigan Medicine, Ann Arbor, MI, USA
[5]Michigan Radiology Quality Collaborative, Ann Arbor, MI, USA
[6]Department of Urology, Michigan Medicine, Ann Arbor, MI, USA
[7]1500 E Medical Center Dr B2-A209P, Ann Arbor, MI 48109, USA

Abstract

Purpose: The purpose of the study is to determine whether a novel semi-automated DIXON-based fat quantification algorithm can reliably quantify visceral fat using a CT-based reference standard.

Methods: This was an IRB-approved retrospective cohort study of 27 subjects who underwent abdominopelvic CT within 7 days of proton density fat fraction (PDFF) mapping on a 1.5T MRI. Cross-sectional visceral fat area per slice (cm^2) was measured in blinded fashion in each modality at intervertebral disc levels from T12 to L4. CT estimates were obtained using a previously published semi-automated computational image processing system that sums pixels with attenuation − 205 to − 51 HU. MR estimates were obtained using two novel semi-automated DIXON-based fat quantification algorithms that measure visceral fat area by spatially regularizing non-uniform fat-only signal intensity or de-speckling PDFF 2D images and summing pixels with PDFF ≥ 50%. Pearson's correlations and Bland–Altman analyses were performed.

Results: Visceral fat area per slice ranged from 9.2 to 429.8 cm^2 for MR and from 1.6 to 405.5 cm^2 for CT. There was a strong correlation between CT and MR methods in measured visceral fat area across all studied vertebral body levels (r = 0.97; n = 101 observations); the least (r = 0.93) correlation was at T12. Bland–Altman analysis revealed a bias of 31.7 cm^2 (95% CI [− 27.1]–90.4 cm^2), indicating modestly higher visceral fat assessed by MR.

Conclusion: MR- and CT-based visceral fat quantification are highly correlated and have good cross-modality reliability, indicating that visceral fat quantification by either method can yield a stable and reliable biomarker.

Key words: Morphometry—Visceral fat—Quantitative imaging—Biomarker—Proton density fat fraction (PDFF)

The increasing incidence of obesity and its concomitant pathology has generated interest in fat quantification as a means to inform patient-specific clinical decision-making [1, 2]. Evidence suggests that adipose tissue is not homogenous, but rather a collection of deposits that vary in their clinical significance and disease implications [3, 4]. Visceral fat—that which specifically surrounds abdominal organs—is believed to possess unique metabolic properties when compared with subcutaneous fat [1–3, 5]. Visceral fat can independently predict disease risk, degree of pathology, procedural outcomes, and mortality related to cardiovascular disease, metabolic syndrome, systemic inflammation, and cancer [1, 2, 6–12]. Encouragingly, visceral fat may also be specifically responsive to lifestyle and pharmaceutical interventions

Correspondence to: Matthew S. Davenport; *email:* matdaven@med.umich.edu

[12]. Therefore, it is increasingly desirable to quantify visceral fat, as distinct from total body mass, for both clinical and research purposes [1, 7, 12].

MRI and CT have been explored as methods of quantifying visceral fat [1, 2, 7, 13, 14]. Although less accessible and more expensive than common anthropomorphic measures of visceral fat (e.g., body mass index (BMI), waist circumference, waist-to-hip ratio, bioelectrical impedance), they are more accurate [7, 15, 16]. Anthropomorphic measures are unable to distinguish visceral fat from other fat deposits [1–3, 5] and may fail to correlate with visceral fat at all [17].

CT-based visceral fat quantification is based on measuring specific Hounsfield unit ranges known to correspond to fat [1, 2]. Generally, single-slice visceral fat area is used as a surrogate for total visceral fat volume to minimize ionizing radiation exposure [2]. While single-slice visceral fat area correlates with abdominal visceral fat volume [5, 14], which may suffice for population studies, variations in fat distribution by gender, ethnicity, disease state, habitus, and other patient demographics may render this approach unreliable for individualized medical decision-making [18]. MRI-based visceral fat quantification also is well-established [10], and is commonly measured using T1-weighted [19] or proton density fat fraction (PDFF) images [1]. However, there is greater variation in MR estimates compared with CT [2] due to signal intensity inhomogeneity, partial volume effects, susceptibility artifacts, and motion artifacts [1, 4]. These complications necessitate additional special image processing [1, 15, 16, 20], for which no standard protocol exists [12].

Since visceral fat is both clinically important and measurable, it represents a potential biomarker by which researchers can compare patient populations and clinicians can inform individualized management plans. However, biomarker usage only is appropriate if measurements are known to be both accurate and precise. It is not well-established whether CT- and MR-based methods offer consistent and interchangeable estimates of visceral fat. Should CT and MR measurements prove interchangeable, researchers and clinicians could choose amongst modalities, making this biomarker more convenient and available without sacrificing reliability. For example, MR may be preferable for visceral fat quantification in pediatric populations, longitudinal studies, or for imaging larger body areas [1]. Body habitus is particularly relevant to the ongoing question of whether single-slice visceral fat area provides an acceptable surrogate measure of total visceral fat volume [5, 14, 18], and if so, which slice level is most appropriate based on gender [5, 21], ethnicity, disease state, and other demographics [18, 22]. Though MR image acquisition may be limited by expense, proton density fat fraction (PDFF)—the most robust method of MR fat quantification [23]—is routinely acquired during abdominal MR exams, making this information freely available from other imaging indications [10].

We sought to determine the correlation between MR- and CT-derived visceral fat estimates by comparing two novel DIXON-based fat quantification algorithms with a previously published CT fat quantification method [24]. The purpose of this study was to determine whether a novel semi-automated DIXON-based fat quantification algorithm can reliably quantify visceral fat using a CT-based reference standard.

Methods

The institutional review board approved this Health Insurance Portability and Accountability Act (HIPAA)-compliant retrospective diagnostic accuracy study. The requirement for informed consent was waived.

Study population

The study population was composed of subjects at the study institution who had undergone both proton density fat fraction (PDFF) mapping at 1.5T and abdominopelvic CT within a 7-day period from 1/1/2015 to 12/31/2016. A maximum of 7 days was chosen to minimize the odds that a subject would undergo significant changes in their visceral fat content between the two examinations. Subjects were identified by query of the institutional radiology information system (RIS) using template report-driven keyword matching. A total of 30 subjects met inclusion criteria. Three subjects were excluded because the paired PDFF data or CT data could not be retrospectively identified for analysis. The final study population was composed of 27 subjects. Study population details are shown in Table 1.

Image acquisition

MR data were acquired using a body coil on one of the two 1.5-Tesla MR machines (Philips, Achieva or Inge-

Table 1. Study population details

Characteristic	Mean (range) or *N* (%)
Age	54 (37–76)
Female	12 (44.4%)
Male	15 (55.6%)
Weight (kg)	84.7 (42.6–124.9)
Height (m)	1.69 (1.54–1.88)
Body mass index (kg/m^2)	29.4 (17.9–40.2)
Hyperlipidemia	7 (25.9%)
Diabetes mellitus	2 (7.4%)
Hypertension	14 (51.9%)
Peripheral vascular disease	0 (0%)
Coronary artery disease	3 (11.1%)
Days between CT and MR	2.5 (0-7)

nia). A commercially available PDFF sequence was obtained in a single breath-hold (generally end expiration). Key acquisition parameters included the following: axial sections encompassing the liver; 3D gradient echo; 6 echoes (TE1 = 0.92 ms, deltaTE = 0.7 ms); TR = 5.3 ms; flip angle = 5°; nominal FOV = 350 × 350 mm ; and quantity of slices (67 nominal) were adjusted to suit body habitus; acquired voxel volume = 3 × 3 × 6 mm^3; reconstructed voxel volume = 1.5 × 1.5 × 3 mm^3; parallel imaging factor = 1.5. Water-only, fat-only, PDFF, and T2* maps were generated online using a 7-peak model that included T2* decay and field inhomogeneity correction.

CT data were acquired in the portal-venous phase in a single breath-hold (generally end expiration) on one of the several 16- or 64-slice multidetector CT scanners (General Electric, HD750 or Lightspeed) with the following settings: tube voltage 120 kV, pitch 1.375, automatic modulation of tube current in proportion to body mass. Images were reconstructed using the following parameters: slice thickness 5 mm, slice interval 1.25, display field of view to fit the patient. Twenty-one subjects received both positive oral and IV contrast (125 mL iopamidol 300). Five subjects received neither oral nor IV contrast.

Visceral fat quantification overview

Cross-sectional visceral fat area per slice (cm^2) was measured in blinded fashion in each modality at intervertebral disc levels from T12 to L4. Not all target levels were spanned by the CT or MR data in some patients because they had been performed for clinical reasons. Vertebral body levels were manually checked for each modality by four coauthors in consensus to confirm accuracy.

CT estimates were obtained using a previously published [24] semi-automated computational image processing system that sums pixels within the visceral peritoneal envelope that have CT numbers − 205 to − 51 HU. There is no international standard definition for this CT number range. The range we used was previously published and likely is a specific (rather than sensitive) estimate of fat pixels. MR estimates were obtained using two novel semi-automated DIXON-based fat quantification algorithms that measure visceral fat area by spatially regularizing non-uniform fat-only signal intensity (MR Method 1) or de-speckling PDFF 2D images (MR Method 2) and summing pixels with PDFF ≥ 50%. A single slice was analyzed at each intervertebral disc level for CT, and three slices were averaged at each intervertebral disc level for MR. The average value of the MR data was compared to the single slice of CT data during analysis.

Visceral fat quantification details: CT

CT images were processed using Analytic Morphomics, a proprietary, semi-automated computational image processing system written in MatLab (The MathWorks, Inc, Natick, MA), that has previously been described [24]. CT scans in DICOM format were imported to the spatial database. First, spinal vertebral levels were identified and labeled in a semi-automated fashion. Next, outer fascial boundaries were traced in a semi-automated fashion and stored as geometry objects, which were reviewed and confirmed prior to estimate extraction. Finally, the algorithm quantified visceral fat as the cross-sectional area of pixels within the visceral peritoneal envelope that have CT numbers − 205 to − 51 HU; intraluminal enteric contents were not excluded. Visceral fat area was measured at intervertebral disc levels from T12 to L4, each from the single slice nearest to the inferior aspect of the stated vertebral body. A representative output is shown in Fig. 1A. The semi-automated process for vertebral body localization was verified manually by four coauthors in consensus.

Visceral fat quantification details: MR

For MR data, available survey scans along with fat-only, water-only, and PDFF DICOM images were converted to 3D Meta-Image format (.mhd) files using in-house MatLab routines. Regions of interest were manually defined within the body wall at intervertebral disc levels from T12 to L4, each from the single slice nearest to the inferior aspect of the stated vertebral body, guided by inspection of orthogonal views in 3D Slicer ver4.6.2. Intramuscular fat and marrow fat were excluded, but intraluminal enteric contents were not (consistent with the CT protocol). Regions of interest were stored as binary masks in.mhd format. Region-of-interest masks, fat-only, and PDFF.mhd files were inputs to in-house MatLab routines to automatically derive visceral fat area at target levels as follows. "Mask1" maps were derived directly from the manually drawn regions of interest where pixels within and outside the body wall were set to 1 and 0, respectively. Next, signal uniformity of thresholded fat-only images was improved by 2D regularization. Within a given slice, fat-only pixels greater than 0.2× their maximum value were regularized to improve uniformity of the fat-only signal intensity over the FOV. Following regularization, mean signal of only those pixels involved in the regularization was calculated. "Mask2" maps were created for each slice where regularized fat-only pixels greater than 0.4 x their average were assigned value 1 with other pixels assigned 0. Finally, "Mask3" was derived from PDFF maps where pixels ≥ 50% fat fraction were assigned 1, with the remainder assigned value 0. A composite mask for each slice was defined as the product of Mask1 × Mask2 ×

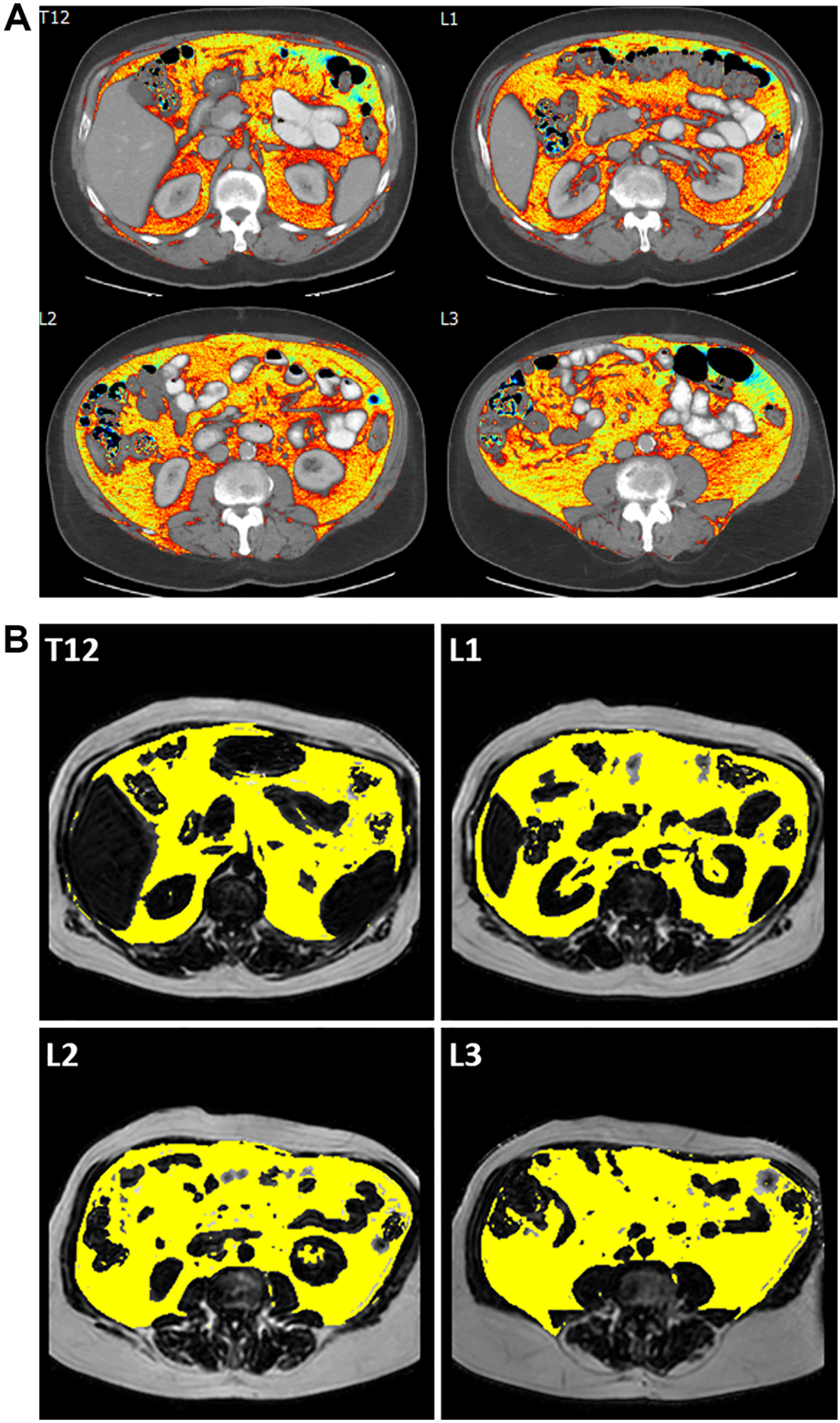
A
T12
L1
L2
L3
B
T12
L1
L2
L3

◀**Fig. 1.** **A** Representative output from the CT visceral fat quantification method (Analytic Morphomics), for subject #5. Colored pixels are those identified as visceral fat, shown here in six axial slices from intervertebral disc levels T12 through L4. **B** Representative output from MR method 1, depicting four axial slices of subject #5 (T12: top left, L1: top right, L2: bottom left, L3: bottom right). Pixels identified as visceral fat are colored yellow. **C** Example process of MR Method 2, depicting unsupervised de-speckling of the quantitative percent fat map for a single axial slice (at T12) of subject #5 (same slice as in top left of **B**). Proton density fat fraction map (a) before and (b) after de-speckling process in which much of the area of "speckle" artifact is removed. PDFF values $> 50\%$ are colorized yellow in (c), and only yellow pixels within the manually drawn body wall region are counted as visceral fat as shown in (d).

Mask3 so that visceral fat area of each slice was estimated by the sum of pixels with value = 1 scaled by pixel area (MR Method 1). A representative output is shown in Fig. 1B.

An alternative fat quantitation algorithm was also applied in MatLab, using locally de-speckled PDFF maps directly to define Mask3 (MR Method 2). In low signal-to-noise regions, water-fat decomposition becomes unstable leading to highly localized (1 to few pixels) PDFF value extremes, referred to as "speckles." Unsupervised spatial de-speckling was performed, assuming randomly and highly varying speckle intensities, using 2D local moving average and standard deviation with automatically determined window width (> 3 points) that depended on the image resolution. The speckles were detected from spatial standard deviation image as exceeding half-width of smoothed high-fat fraction whole volume histogram (between 50% and 100% fat with 2% bin-size). For windows > 3 points, two iterations were applied with optimal and 2-point lower window width using 1D directional-window smoothing probe for pixel set different between windows. The detected speckles were masked off the PDFF before Mask3 was determined and visceral fat area estimated as

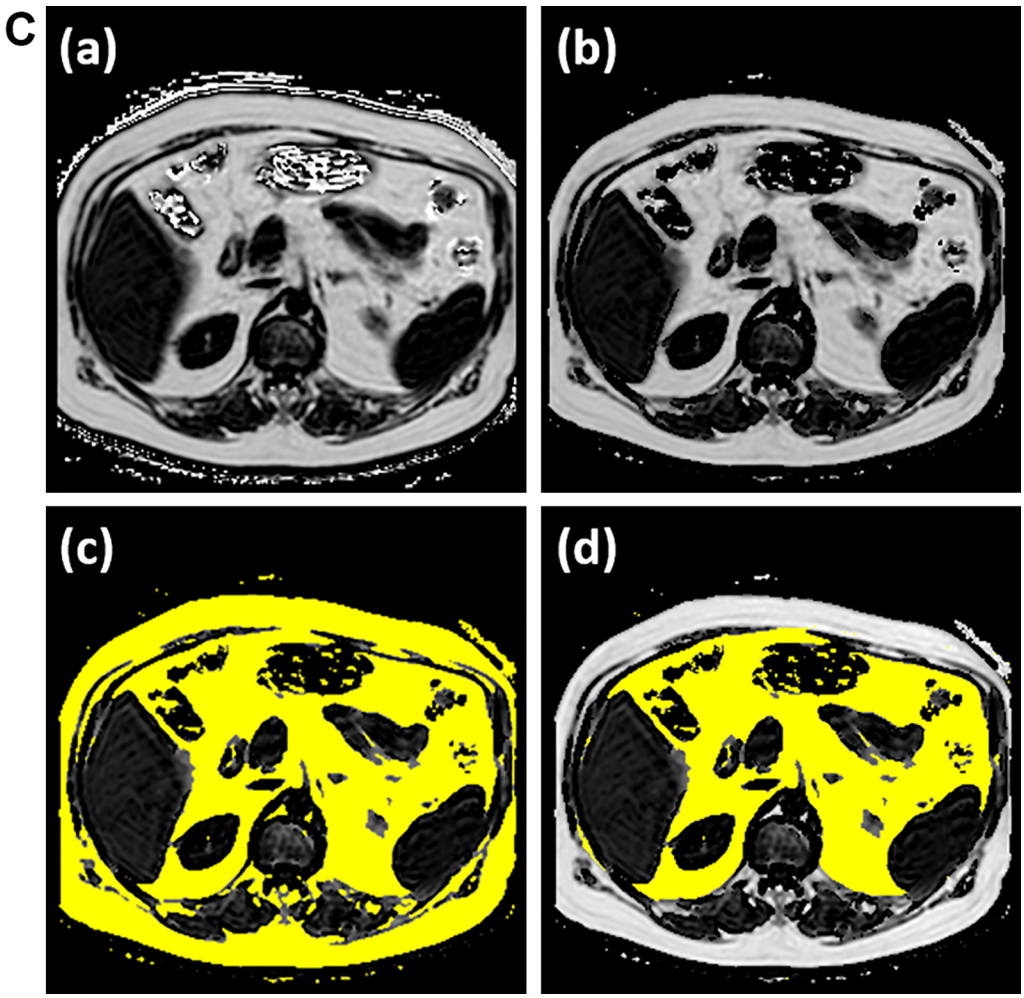

Fig. 1. continued.

described above for MR Method 1. An example of the de-speckling process is depicted in Fig. 1C.

Data analysis

Categorical data were analyzed with counts and percentages. Continuous data were summarized with means and ranges. Pearson's correlations were assessed overall and at each vertebral body level comparing both MR methods for measuring visceral fat with the CT method. Bland–Altman analyses were performed comparing both MR methods with the CT method. Bias and 95% confidence intervals were calculated.

Results

The study population details are shown in Table 1. The mean length of time separating the MR and CT examinations was 2.5 days (range 0–7 days). Visceral fat area per slice ranged from 9.2 to 429.8 cm^2 for MR and from 1.6 to 405.5 cm^2 for CT. The number of slice observations with CT and MR data available at the inferior endplate of each vertebral body level was total (n = 101), T12 (n = 27), L1 (n = 25), L2 (n = 23), L3 (n = 18), L4 (n = 8).

Average visceral fat area per slice (cm^2) were strongly correlated between CT and MR methods (MR method 1 and CT: r = 0.967; MR method 2 and CT: r = 0.965; Table 2, Fig. 2A–D). The correlations were greatest at the inferior endplate of L3 (Method 1: r = 0.979; Method 2: r = 0.982) and lowest at the inferior endplate of T12 (Method 1: r = 0.931; Method 2: r = 0.924) (Table 2).

MR-based estimates of visceral fat area were systematically higher than CT-based estimates (Fig. 3A–C) with average bias of 31.7 cm^2 for MR method 1 (Fig. 3A, 95% confidence interval [− 27.1] to 90.4 cm^2) and 36.4 cm^2 for MR method 2 (Fig. 3B, 95% confidence interval [− 23.4] to 96.3 cm^2). There was negligible bias of − 4.8 cm^2 between the two MR methods (Fig. 3C, 95% confidence interval [− 16.0] to 6.5 cm^2). The MR–CT and MR–MR systematic biases did not vary over the range of visceral fat areas we measured (Fig. 3A, B).

Table 2. Correlation matrix of average visceral fat area/slice (cm^2) assessed by MR methods 1 and 2 vs. CT method

Vertebral body level	MR method 1 vs. CT	MR method 2 vs. CT
T12	0.931	0.924
L1	0.975	0.974
L2	0.973	0.973
L3	0.979	0.982
L4	0.963	0.963
All levels	0.967	0.965

Data are Pearson's r

Discussion

Visceral fat cross-sectional areas measured by MR and CT were highly correlated with excellent cross-modality reliability. There was a consistent positive bias for MR-based methods of visceral fat quantification compared with CT (31.7–36.4 cm^2) that did not vary over the range of values we studied, indicating consistently greater visceral fat areas measured by MR. However, the bias value confidence intervals for both MR methods include zero, indicating that the bias may have no significance. Any existing bias may be due to thresholding effects related to the included range of CT numbers (− 205 to − 51 HU) and could potentially be eliminated or reduced by increasing the sensitivity of the CT number range. An alternative possibility is that the difference was due to differences in de-speckling or smoothing routines. In either case, the bias was consistent across the range of values we studied, indicating that corrected values of visceral fat quantification by either MR or CT can provide a stable and cross-modality reliable estimate of visceral fat. This has potential value because visceral fat is linked to important health outcomes (e.g., cardiovascular disease) and often is incidentally imaged by CT and MR performed for unrelated clinical indications.

Several studies have demonstrated good correlation between MR and CT estimates of visceral fat [1, 20, 25–28]. One study of seven subjects, done in 1990 by Seidell et al. [20], was the only one we identified that found considerably different estimates between CT and MR methods, possibly attributable to partial volume effects and early MR imaging technology. In 2012, Klopfenstein et al. [25] compared single-slice visceral fat estimates from same-day MR and CT of 27 subjects in a longitudinal study of polycystic ovarian syndrome and found strong agreement between modalities (Pearson's r = 0.89) with mean bias of − 2.9% (MR vs. CT). In 2005, Gomi et al. [26] showed no significant difference in visceral fat estimates obtained between single-slice MR and single-slice CT. In 2009, Kullberg et al. [27] found good correlation between MR- and CT-based estimates, though MR slightly underestimated visceral fat compared to CT. Visceral fat quantification has been extended to other imaging modalities as well. In a 2001 study of 19 subjects, Stolk et al. [28] found good correlation of ultrasound estimates with single-slice CT- and MR-based methods (Pearson's r = 0.81 and r = 0.83, respectively), but did not compare the CT and MR methods directly. Finally, the repeatability of fat quantification between images has been researched. In 2017, Middleton et al. [29] explored the repeatability of semi-automated MR-based abdominal adipose tissue quantification in a prospective study of 20 subjects and found that MR-based visceral fat quantification with partial volume correction was highly repeatable and accurate over three same-day images; however, no comparison to

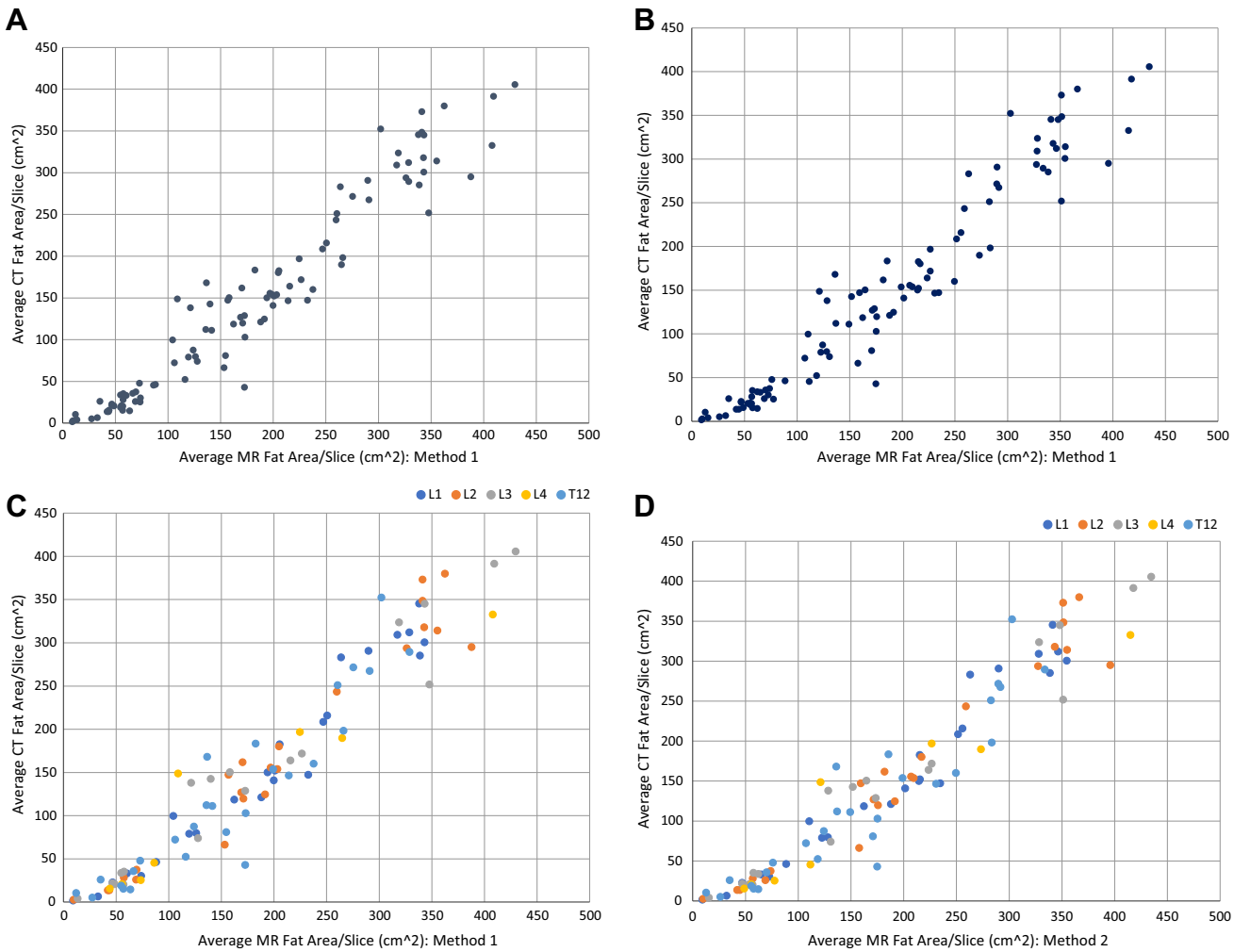

Fig. 2. **A** Scatter plot of average visceral fat area/slice (cm^2) assessed by MR method 1 (x-axis) and CT (y-axis). All slice levels from T12 to L4 included. Pearson's $r = 0.967$. **B** Scatter plot of average visceral fat area/slice (cm^2) assessed by MR method 2 (*x*-axis) and CT (*y*-axis). All slice levels from T12-L4 included. Pearson's $r = 0.965$. **C** Scatter plot of average visceral fat area/slice (cm^2) by vertebral body level assessed by MR method 1 (*x*-axis) and CT (*y*-axis). **D** Scatter plot of average visceral fat area/slice (cm^2) by vertebral body level assessed by MR method 2 (*x*-axis) and CT (*y*-axis).

CT was made. In general, our study agrees with the findings of these other investigators and demonstrates reliability at multiple slice levels with two different MR methods of quantification.

We found systematically greater values of visceral fat by using MR-based quantification compared to CT-based quantification. This finding may be attributable to the chosen CT fat thresholds and probably could be eliminated or reduced by expanding the CT number range used to indicate the presence of fat (e.g., using an upper bound that is somewhere between − 51 and − 10 HU [30]). We did not explicitly test which thresholds would provide the greatest level of absolute agreement, but the lack of variation in the levels of bias across the range of values we studied suggests that a simple correction may be all that is necessary. Both MR-based methods we studied produced consistent results with minimal cross-method bias (− 4.8 cm^2).

The results of this study are limited by inconsistent slice selection between MR and CT. Patients were naturally in slightly different positions, and imaging slices were not necessarily performed exactly at the same level or on the same day. Additionally, threshold values for visceral fat could hypothetically be affected by variability in contrast material dynamics. The consistency of the results between CT and MR imaging despite mean separation of 2.5 days and some variability in imaging protocol (e.g., with or without oral or IV contrast) is encouraging. Further study investigating optimal threshold values for CT-based quantification is warranted. Estimates were obtained with each operator blinded to the results of the other, but we might have

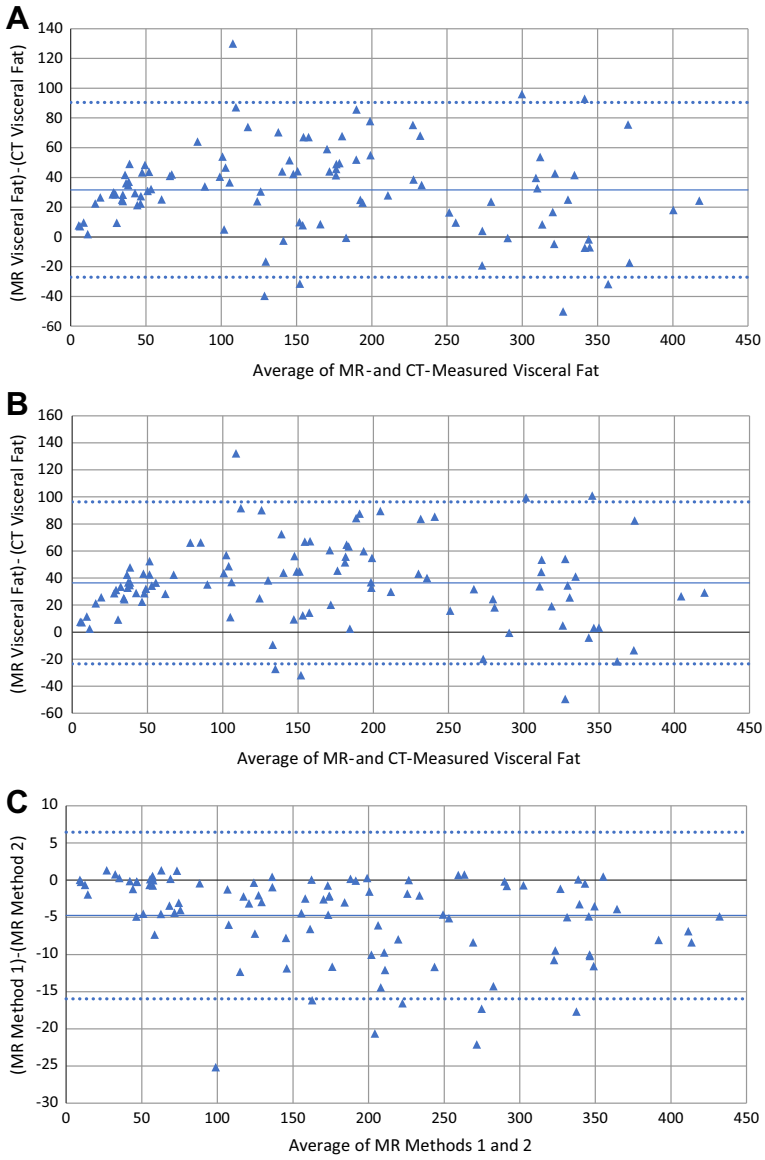

Fig. 3. **A** Bland–Altman plot of average visceral fat area/slice (cm^2) assessed by MR method 1 and CT. All slice levels from T12 to L4 included. Solid line is bias (31.7 cm^2), indicating higher average areas assessed by MR method 1 compared to CT. Dotted lines are upper (90.4 cm^2) and lower (− 27.1 cm^2) 95% confidence intervals. **B** Bland–Altman plot of average visceral fat area/slice (cm^2) assessed by MR method 2 and CT. All slice levels from T12 to L4 included. Solid line is bias (36.4 cm^2), indicating higher average areas assessed by MR method 2 compared to CT. Dotted lines are upper (96.3 cm^2) and lower (− 23.4 cm^2) 95% confidence intervals. **c.** Bland–Altman plot of average visceral fat area/slice (cm^2) assessed by MR method 1 and MR method 2. All slice levels from T12 to L4 included. Solid line is bias (− 4.8 cm^2), indicating higher average areas assessed by MR method 2 compared to MR method 1. Dotted lines are upper (6.5 cm^2) and lower (− 16.0 cm^2) 95% confidence intervals. Note scale change compared to the MR vs. CT Bland–Altman plots.

observed different results if additional operators were included. Intraluminal bowel contents were not excluded from the analysis. Therefore, ingested fatty foods or steatorrhea could contribute error to our estimates. Finally, while single-slice areas are commonly used to represent the quantity of visceral fat, further study with 3D volumes could be considered to determine if they better predict important health outcomes.

In conclusion, MR- and CT-based visceral fat quantification methods are highly correlated and have good cross-modality reliability, indicating that visceral fat quantification by either method can yield a stable and reliable biomarker. Future work should include investigation of 3D volume estimates, determining optimal CT thresholding values (e.g., by determining which CT number range best matches the MR data), demonstrating

applicability in larger patient populations, and linking these biomarker data to specific health-related outcomes.

Compliance with ethical standards No funding was solicited or used for this work. Institutional review board approval was obtained. The requirement for informed consent was waived by the IRB. All procedures performed in studies involving human participants were in accordance with the ethical standards of the institutional and/or national research committee and with the 1964 Helsinki Declaration and its later amendments or comparable ethical standards.

Financial disclosure Matthew Davenport—Royalties from Wolters Kluwer, Katherine M. Heckman—No conflict of interest, Bamidele Otemuyiwa—No conflict of interest, Thomas L. Chenevert—No conflict of interest, Dariya Malyarenko—No conflict of interest, Brian A. Derstine—No conflict of interest, Stewart C Wang—No conflict of interest.

References

1. Garg K, Chang S, Scherzinger A (2013) Obesity and diabetes: newer concepts in imaging. Diabetes Technol Ther 15:351–361
2. Shuster A, Patlas M, Pinthus JH, et al. (2012) The clinical importance of visceral adiposity: a critical review of methods for visceral adipose tissue analysis. Br J Radiol 85:1–10
3. Balentine CJ, Marshall C, Robinson C, et al. (2010) Validating quantitative obesity measurements in colorectal cancer patients. J Surg Res 164:18–22
4. Shen W, Wang Z, Punyanita M, et al. (2003) Adipose tissue quantification by imaging methods: a proposed classification. Obes Res 11:5–16
5. Furukawa K, Katabami T, Nakajima Y, et al. (2010) Evaluation of a whole-abdominal fat volume by 700-slice CT scanning and comparison with the umbilical fat area anthropometric indices. Obes Res Clin Pract 4:111–117
6. Demerath EW, Reed D, Rogers N, et al. (2008) Visceral adiposity and its anatomical distribution as predictors of the metabolic syndrome and cardiometabolic risk factor levels. Am J Clin Nutr 88:1263–1271
7. Doyle SL, Bennett AM, Donohoe CL, et al. (2013) Establishing computed tomography-defined visceral fat area thresholds for use in obesity-related cancer research. Nutr Res 33:171–179
8. Abdelbadee AY, Paspulati RM, McFarland HD, et al. (2016) Computed tomography morphometrics and pulmonary intolerance in endometrial cancer robotic surgery. J Minim Invas Gynecol 23:1075–1082
9. Locke JE, Carr JJ, Sangeeta N, et al. (2017) Abdominal lean muscle is associated with lower mortality among kidney waitlist candidates. Clin Transplant 31:e12911
10. Sabel MS, Terjimanian M, Conlon ASC, et al. (2013) Analytic morphometric assessment of patients undergoing colectomy for colon cancer. J Surg Oncol 108:169–175
11. Van Der Sloot KWJ, Joshi AD, Bellavance DR, et al. (2017) Visceral adiposity, genetic susceptibility, and risk of complications among individuals with Crohn's disease. Inflamm Bowel Dis 23:82–88
12. Demerath EW, Shen W, Lee M, et al. (2007) Approximation of total visceral adipose tissue with a single magnetic resonance image. Am J Clin Nutr 85:362–368
13. Schweitzer L, Geisler C, Pourhassan M, et al. (2015) What is the best reference site for a single MRI slice to assess whole-body skeletal muscle and adipose tissue volumes in healthy adults? Am J Clin Nutr 102:58–65
14. Shen W, Punyanitya M, Wang Z, et al. (2004) Total body skeletal muscle and adipose tissue volumes: estimation from a single abdominal cross-sectional image. J Appl Physiol 97:2333–2338
15. Bosy-Westphal A, Later W, Hitze B, et al. (2008) Accuracy of bioelectrical impedance consumer devices for measurement of body composition in comparison to whole body magnetic resonance imaging and dual X-ray absorptiometry. Obes Facts 1:319–324
16. Stewart KJ, DeRegis JR, Turner KL, et al. (2003) Usefulness of anthropometrics and dual-energy x-ray absorptiometry for estimating abdominal obesity measured by magnetic resonance imaging in older men and women. J Cardiopulm Rehabil 23:109–114
17. O'Connor M, Ryan J, Foley S (2015) Best single-slice location to measure visceral adipose tissue on paediatric CT scans and the relationship between anthropometric measurements, gender and VAT volume in children. Br J Radiol 88:20140711
18. Lee S, Kuk JL, Kim Y, et al. (2011) Measurement site of visceral adipose tissue and prediction of metabolic syndrome in youth. Pediatr Diabetes 12:250–257
19. Li X, Youngren JF, Hyun B, et al. (2008) Technical evaluation of in vivo abdominal fat and IMCL quantification using MRI and MRSI at 3T. Magn Reson Imaging 26:188–197
20. Seidell JC, Bakker CJG, van der Kooy K (1990) Imaging techniques for measuring adipose-tissue distribution—a comparison between computed tomography and 1.5T magnetic resonance. Am J Clin Nutr 51:953–957
21. Kuk JL, Church TS, Blair SN, et al. (2010) Measurement site and the association between visceral and abdominal subcutaneous adipose tissue with metabolic risk in women. Obesity 18:1336–1340
22. Shen W, Punyanitya M, Chen J, et al. (2007) Visceral adipose tissue: relationships between single slice areas at different locations and obesity-related health risks. Int J Obes 31:763–769
23. Reeder SB, Hu HH, Sirlin CB (2012) Proton density fat-fraction: a standardized MR-based biomarker of tissue fat concentration. J Magn Reson Imaging 36:1011–1014
24. Stidham RW, Waljee AK, Day NM, et al. (2015) Body fat composition assessment using analytic morphomics predicts infectious complications after bowel resection in Crohn's disease. Inflamm Bowel Dis 21:1306–1313
25. Klopfenstein BJ, Kim MS, Krisky CM, et al. (2012) Comparison of 3T MRI and CT for the measurement of visceral and subcutaneous adipose tissue in humans. Br J Radiol 85:826–830
26. Gomi T, Kawawa Y, Nagamoto M, et al. (2005) Measurement of visceral fat/subcutaneous fat ratio by 0.3 Tesla MRI. Radiat Med 23:584–587
27. Kullberg J, Brandberg J, Angelhed JE, et al. (2009) Whole-body adipose tissue analysis: comparison of MRI, CT and dual energy X-ray absorptiometry. Br J Radiol 82:123–130
28. Stolk RP, Wink O, Zelissen PMJ, et al. (2011) Validity and reproducibility of ultrasonography for the measurement of intra-abdominal adipose tissue. Int J Obes 25:1346–1351
29. Middleton MS, Haufe W, Hooker J, et al. (2017) Quantifying abdominal adipose tissue and thigh muscle volume and hepatic proton density fat fraction: repeatability and accuracy of an MR imaging-based semiautomated analysis method. Radiology 283:438–449
30. Davenport MS, Neville AM, Ellis JH, et al. (2011) Diagnosis of renal angiomyolipoma with Hounsfield unit thresholds: effect of size of region of interest and nephrographic phase imaging. Radiology 260:158–165